Natural laminar flow leading edge: Requirements, design, and experimental validation under operational loads

Olaf Steffen[a,*], Patrick Meyer[b], Christian Hühne[a,b]

[a]German Aerospace Center DLR, Institute of Lightweight Systems, Lilienthalplatz 7, 38108 Braunschweig, Germany
[b]Technische Universität Braunschweig, Institute of Mechanics and Adaptronics, Langer Kamp 6, 38106 Braunschweig, Germany

Abstract

To unlock the potential of natural laminar flow aircraft wings, novel structural designs are necessary for the wing leading edge and its attachment. Those designs may not impinge on operability and maintenance of the aircraft. This paper presents a leading edge and attachment design for the natural laminar flow environment as well as the testing of this design on a large-scale ground-based demonstrator. The leading edge design is numerically verified by considering operational loads. For operational viability, the replacement of damaged leading edges without alterations to the spare part is desirable. In a series of tests, such interchange trials are made with two 2.3 m full complexity leading edge segments and the aerodynamic step height at the interface of leading edge and wing cover is assessed in both ground and cruise deformation. The leading edge design and its attachment concept were proven to support natural laminar flow step height requirements even under global part deformations of a multi-material structure under thermal loading both numerically and experimentally. Interchangeability of the leading edge is demonstrated with very low mean variation in step height between different installations.

Keywords: natural laminar flow, large-scale testing, wing design, wing leading edge, laminar flow wing, aircraft operation

1. Introduction

Economic needs and a growing ecological awareness demand a cut in aircraft fuel consumption to reduce CO2 emissions and operation costs. The fuel consumption of aircraft can be decreased by improving the aircraft's aerodynamics. A long-discussed approach for improving efficiency is to sustain laminar flow over large surface areas of a transport aircraft. Laminar flow research with the focus on aircraft application dates back as far as the 1930s [1]. With a contribution of about 18% to the aircraft's total friction drag of a typical transport aircraft [2], the wing is mostly suited for laminar flow application. The reduced friction drag of a natural laminar flow (NLF) wing can lead to a reduction in fuel consumption and thus reduction of CO2 emissions by up to 8% [3]. However, laminar flow is sensitive to surface disturbances. Steps, gaps and surface waviness can trigger early laminar–turbulent transition [4, 5]. Research on laminar flow in flight tests was mostly dedicated to the determination of aerodynamic parameters or the validation of aerodynamic models. However, the structures used were not representative and were only surrogates, like laminar gloves on conventional wing structures [1, 6]. With the BLADE flight test campaign, laminar flow research has entered a new era with the application of airframe structures developed explicitly for laminar flow research. However, even those structures are supposed to serve as proofs of concept, being representative of a possible laminar wing structure [7] neglecting some operational aspects such as removable leading edges, erosion protection or wing ice protection systems.

With exception of the *HondaJet*, no dedicated laminar wing structures are operational today in commercial applications. The wing covers of the HondaJet are milled from a solid block of aluminium and include all stringers and rib attachments [8]. Thus, a surface compatible with laminar flow requirements can be achieved. However, the wing architecture of a business jet aircraft is far less complex compared to a large passenger aircraft, with no movable leading edge (LE) high-lift device needed on most business jets. NLF on large passenger aircraft is still an exception, until today only applied to smaller surfaces, like on the vertical tail plane of the Boeing 787 as hybrid laminar flow [9]. On the wing, large transport aircraft use high-lift wing devices to allow higher angles of attack and increase lift. LE high-lift devices are typically extendable slats on top of fixed LEs. Those slats create a discontinuity on to wing surface detrimental to laminar flow. Conventional designs make regular use of fasteners through the wing and LE skins to join them with ribs, especially at the interface between fixed LE and upper cover. Executed as a lap joint, this interface may also show steps between the parts that are incompatible with NLF when no measures are taken to compensate for thickness variation in the composite parts joined. To avoid these flow disturbances

Abbreviations: BFS, backward-facing step; CFRP, carbon-fibre-reinforced plastic; CTE, coefficient of thermal expansion; FEA, finite element analysis; FFS, forward-facing step; GBD, ground-based demonstrator; GFRP, glass-fibre-reinforced plastic; LE, leading edge; NLF, natural laminar flow; UD, unidirectional; WIPS, wing ice protection system.

*Corresponding author.
Email addresses: olaf.steffen@dlr.de (Olaf Steffen), pat.meyer@tu-braunschweig.de (Patrick Meyer), christian.huehne@dlr.de (Christian Hühne)

experienced with conventional wing designs, a new structural design approach is needed for a NLF wing.

The BLADE aircraft features two different designs on the right and the left wing [10]. The left-hand wing designed and produced by Saab uses an integrated LE and integrated ribcaps on the wing skin's upper cover [11]. Thus, steps and fastener heads on the outside are avoided and a very clean surface is created. Wing cover and LE form a single composite part. The right-hand wing LE also has integrated ribcaps for connection with the LE ribs on the inside of the structure. The joint between the LE and the upper cover features fastener heads through the outer surface in a single lap joint. The aerodynamic surface is recovered after installation.

In his overview of the BLADE activities and concept in 2010, Hansen [7] stressed the following as being a key concern within laminar flow wing structural design: an integrated LE may be ideal for laminar flow, but a detachable LE provides operational advantages regarding repair and system's accessibility. Wicke et al. [12] have shown the importance of maintenance cost for the economics of a NLF aircraft operation design. This leads to the need for an interface between the wing upper cover and the LE that does not negatively affect the boundary layer transition line but is not overly complicated to produce, assemble and maintain. Such operational aspects remain unaddressed in the literature regarding the design of NLF structures.

This paper aims to demonstrate the ability to meet tight NLF surface criteria with modern composite designs and reliable repeatability of high-accuracy installation of a LE structure as a means to highlight the maturity of NLF designs for real-life applications. The use case for NLF is cruise flight. For given aerodynamic requirements, the structural design and test process of the structure aim to demonstrate compliance with the NLF requirements for cruise flight. To this end, a multi-material composite wing LE and its NLF-compliant attachment are developed, numerically verified, hardware built and tested in a ground-based demonstrator (GBD). The demonstrator is evaluated under operational load with respect to NLF requirements for the interface between LE and wing cover and interchangeability of the LE. The work focuses on a left-hand wing, with the numerical activities covering a 4.5 m span outer segment (Fig. 1). The wing components are sized towards ultimate load conditions using different manoeuvre load cases. The 2.3 m GBD demonstrator represents a section of the modelled segment, where only the relevant cruise flight deformations are applied to validate the use case.

To deliver a NLF compatible design, the various requirements and challenges for an NLF leading from overall aircraft concept, aerodynamic requirements, and composite part-specific phenomena are presented and translated into a design concept. With a focus on the joint, the laminate selection, and the rib attachment, a detailed design is presented. The design is validated on the GBD with LE installation and interchange trial series using two 2.3 m long LEs. Installations are made in both a neutral position and a position comparable to a free-cantilevered wing of an aircraft standing on ground. For each installation, aerodynamic step heights between LE and wing cover are measured to assess the NLF compliance.

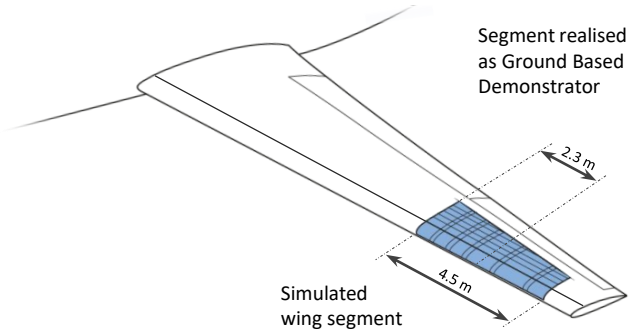

Figure 1: Approximate location of the investigated wing segment (blue) on a left-hand wing. The full 4.5 m long wing segment is investigated numerically, whereas half of the segment is realised in a GBD.

The paper is structured as follows: The requirements are structured as external environmental condition driven requirements and requirements related to the aircraft concept (Section 2). Based on this, the conceptual design and engineering details for key features of the NLF LE are presented (Section 3). The numerical verification of the concepts (Section 4) follows a stepwise approach: for the full LE segment, a suitable layup is selected based on the performance under relevant load cases. The configuration is then verified for adverse LE installation conditions in extreme temperature scenarios at the borders of the design envelope. The validation (Section 5) is led by a summary of the development of a test rig capable to achieve the desired GBD deformations. The main focus of this section is placed on presenting the results for the step height between LE and wing cover achieved in the installation and interchange trials.

2. Requirements for a natural laminar flow leading edge

The requirements for the design of the NLF LE are defined by the aircraft design mission and its environmental factors including aerodynamic requirements to allow NLF on the wing surface. The set of requirements presented is (by far) not exhaustive from an aircraft manufacturer's point of view. However, it represents the boundary conditions applied in the design of the NLF LE investigated within this work. The requirements are summarised in Table 1.

2.1. Requirements from environmental conditions

The design of the LE is strongly driven by the conditions of its operating environment. Temperature range, including icing conditions, lightning, eroding agents and bird strike are influencing factors required to be addressed. The LE experiences a range of different temperatures during operation and manufacturing, as shown in Fig. 2. Next to the outside temperature of −56 °C given by the standard atmosphere at cruise flight altitude, structure temperatures on ground can extend from −70 °C in arctic conditions to up to 90 °C on airfields in arid regions [13]. The temperature envelope is further expanded by the production process of modern aerospace composites, with curing temperatures ranging up to 180 °C for common aerospace thermoset materials.

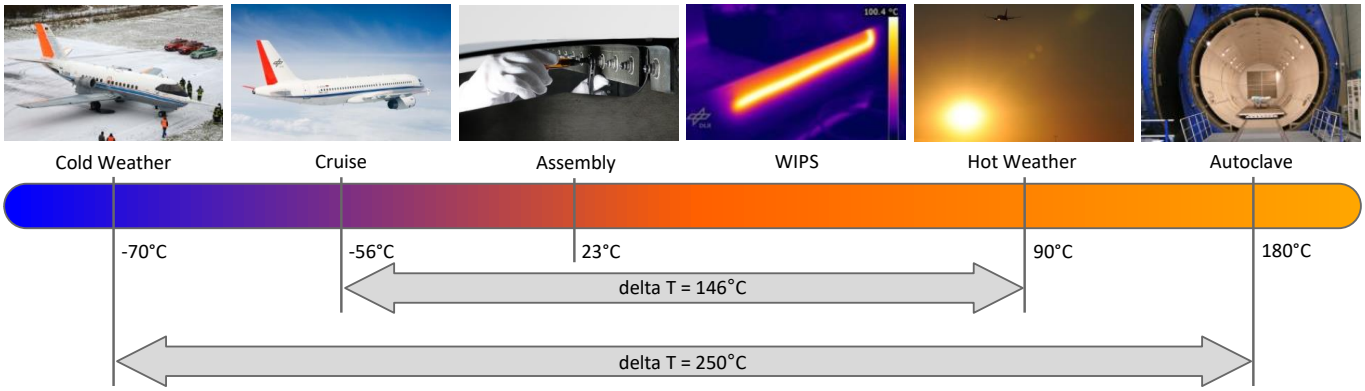

Figure 2: Temperature range experienced by a composite part in its lifecycle.

In combination with atmospheric water content, icing conditions can be present that potentially impact aircraft performance [14]. Therefore, large passenger aircraft have to take measures to prevent undesired changes to flight characteristics. To achieve this, a wing ice protection system (WIPS) is required. To protect the LE from the catastrophic effects of lightning, the LE has to be able to deal with the electrical current resulting from a lightning strike [14].

At fast travel speeds of large passenger aircraft, particles in the air can erode surfaces. This is not only relevant for solid particles, like sand, but also for water droplets. Erosion poses not only a challenge for part longevity but also NLF due to roughness increase. Thus wing LEs need to be protected against erosion if NLF is desired [15]. The LE structure has to be able to deal with the impact of birds in flight to "assure capability of continued safe flight and landing of the aeroplane" according to the EASA CS-25 [14]. Damage to the LE can be accepted. The main focus is to protect the wing box front spar. A bird strike can be one of the possible events necessitating a LE exchange. A specific LE skin thickness minimum of 5 mm is given as a quantitative requirement for the design.

2.2. *Requirements related to the aircraft concept*

From the aircraft concept, relevant requirements for the design of the laminar LE are derived. The overall wing concept defines the LE high-lift device. While conventional slats are considered adversely to sustained NLF, most NLF wing concepts use Krueger flaps as a high-lift device. This provides also shielding against insect contamination while deployed and provides the possibility to design an upper wing surface free of large disturbances. For the design presented in this paper, a Krueger flap is defined as the default high-lift device at the LE. This also enables general access to the joint area between wing upper cover and LE when the Krueger flap is deployed.

The width of a high-lift device section in spanwise direction is determined as a trade-off of following the curvature of the wing and the increasing weight added by high-lift kinematics and drives necessary for additional high-lift device section. The LE section width conforms to the high-lift section. In the concept discussed within this work, the LE section width is defined as 4.5 m on aircraft level and 2.3 m for the demonstrator. Despite all assumed differences between a laminar LE design and a conventional design, the replacement of a damaged LE must not take an excessive amount of time and labour to not impact the business case of an NLF aircraft. Thus the LE exchange is required to be achievable within one night shift [16] without the need for a complex rig to unload the wing. Rework on a replacement LE is not permitted in the scope of this work: LEs need to be interchangeable.

The character of the wing exploiting the lower drag of an NLF boundary layer is also rooted in the overall aircraft concept. Laminar boundary layers are very sensitive to the effects of local surface disturbances. These are typically defined as steps, gaps, waviness, and surface roughness. The latter includes 3d disturbances like fastener heads or insect contamination. The surface disturbances' parameters, like step height, gap width and ratio of amplitude to wavelength, were early covered by handbook formula derived from flight experiments by Carmichael [4] and Nenni and Gluyas [5]. As a result of these experiments, beneficial forms of steps are known [17]. The handbook formulae are known to be conservative for realistic transition prediction for shaped steps [18], e.g., when using fillers to create ramps. Typical surface disturbances at the interface between two assembled components are shown in Fig. 3. Backward facing steps are generally considered to be more critical compared to forward facing steps due to adverse pressure gradients. More precise transition predictions are possible using computational methods nowadays. The boundary layer transition and effect of surface disturbances are dependent on the location of the disturbance on the wing profile. Since most computational methods with higher accuracy tend to have long computation times and are thus equally costly, a wide screening of potential shapes, heights and preferable locations of flow disturbances like component interfaces for different flight conditions of an aircraft concept is still impractical. Only recently faster methods have emerged [19, 20], potentially enabling a broader survey of surface disturbances to enable inclusion in a closed-loop NLF wing design or manufacturing engineering process. They are, however, at the moment restricted to two-dimensional simulations. Thus, allowable step heights remain the prime parameter to evaluate the quality of an interface between two components on an NLF surface.

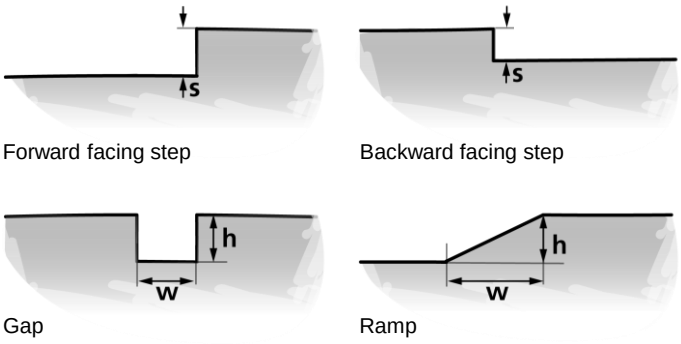

Figure 3: Typical surface disturbances at the interface between two assembled components.

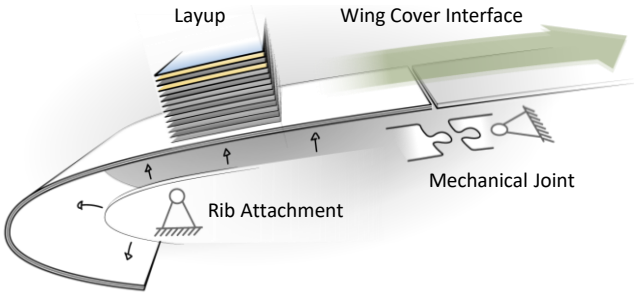

Figure 4: Key development areas for the NLF leading edge.

Since the scope of this work is focused on the structural design of the interface between the LE and the wing upper cover, waviness as an extended surface feature is not considered. 3d disturbances, step heights, and gaps are required to be minimised. Within this work for the specific joint location, a requirement of 0.5 mm forward-facing step (FFS) and −0.1 mm backward-facing step (BFS) is given. Values are derived using aforementioned handbook formulae. Those boundary conditions serve as central aerodynamic requirements and measure of success of the design process and of the ground based demonstrator. The gap at the LE interface is defined to be filled and thus no quantitative gap width requirement is given. A 70° sidewall angle of the gap is defined to be required to enable a successful filling of the gap of the joined components.

The LE structure is to be made out of a carbon-fibre-reinforced plastic (CFRP) material. This is a wing-level design decision acting as a requirement for the LE, with wide implications for the detailed design.

3. Multi-material laminar leading edge design

The wing in scope of the development is a left-hand NLF wing of a medium-range large transport aircraft. The outer wing segment (Fig. 1) is considered in detail, with the GBD being the inner half of the outer wing segment. The wing is considered to have a Krueger flap high-lift device also serving as an insect shield to the LE through take-off and landing. Four sets of challenges can be identified on the LE that have to be addressed to enable laminar flow. Figure 4 illustrates the joint to the upper cover and the gap area, the attachment of the LE to the rib and the multi-material layup.

The requirements for erosion protection, WIPS integration a CFRP structure, in combination with the thermal environment described in Section 2 lead to an attachment design different to the state of the art. To support laminar flow over the LE and the joint, fastener heads on the outside of the structure will be avoided, with the exception of areas where two LE segments meet and a turbulent wedge in the airflow is expected anyway. The concept further allows for LE global deformation, while avoiding local waviness. Higher accuracy through rigid joints is only prioritised where NLF or other functional requirements make it necessary. Fastener loads are also reduced by allowing thermo-elastic deformation. Fewer fasteners also allow for faster exchange of a damaged LE. A first iteration of the LE concept described in this section has been introduced in [21].

3.1. Multi-material, multi-functional laminate

The requirements regarding erosion resistance, lightning and ice protection lead to the design of the LE as a multi-material, multi-functional structure. Composite materials show a weak erosion resistance [22, 23] when unprotected. CFRP components are also prone to damage by lightning strikes due to the material's low electrical conductivity and need lightning strike protection [24, 25]. A steel foil is selected to enhance the erosion characteristics of the LE. It is a design choice common for modern composite wing LEs, for example, also applied to the B787 Dreamliner [26]. Based on impact trials, the thickness of the steel foil erosion protection on the outer surface is selected to be 0.125 mm [27]. This steel foil thickness has proven to meet erosion protection requirements, too [28]. While commonly metallic meshes are used on composite airframe surface components, the steel foil also carries the function of lightning protection, where only a sheet thickness of 0.025 mm would be required [25].

An electro-thermal system is selected for the WIPS. This decision is deemed considerate regarding the trend to more electrical aircraft and efficient propulsion, avoiding engine bleed air as a heating source [26]. Also, high temperatures on the inside of the structure necessary to deliver the power needed for anti- and de-icing on the LE's outer surface are avoided, as high temperatures can be damaging to composite materials. The WIPS consists of an electrically contacted CFRP layer embedded in an isolating glass-fibre-reinforced plastic (GFRP) structure with a total thickness of 0.706 mm. Within the demonstration, the WIPS is only considered as part of the LE's overall composite layup. The functional integration of the WIPS is out-of-scope, has however been successfully demonstrated [29] in anti-icing tests conducted in an icing wind tunnel.

The investigated multi-material LE structure is an enhanced design of the structure presented by Düring et al. [27] applying two modifications. As they are structurally compatible and permanently bonded to the CFRP structure, the WIPS and erosion protection are considered load-carrying and thus counted towards the minimum structural thickness of 5 mm defined as bird strike requirement. With the CFRP base structure built out of 16

Table 1: Requirements overview.

Requirement	Description	Quantity
structural LE material	CFRP	
ice protection	thermal WIPS	
bird strike	min. structural thickness	5 mm
erosion protection	steel erosion shield	
lightning protection	means of diverting electrical current	
aerodynamic NLF	minimal steps	0.5 mm FFS, 0.1 mm BFS
aerodynamic NLF	minimise 3d disturbances	
aerodynamic NLF	gap filled	70° sidewall angle
LE high-lift device	Krueger flap	
max hole position deviation	position deviation from nominal	0.5 mm
interchangeability	one night shift, no rework	7.5 h

unidirectional (UD) layers with a layer thickness of 0.262 mm, the total LE thickness is 5.023 mm. This leads to a thickness reduction from initially 5.931 mm as in [27] to 5.023 mm coming along with a mass reduction of about 14% for the LE structure. Second, ±45° fabric layers used by Düring et al. will be replaced by 45° and −45° UD layers that are applicable for the automated fibre placement (AFP) process. However, coupling effects between bending and twist appear in unsymmetrical but balanced laminates due to different distances of 45° and −45° layers from the laminate's mid-plane.

With the multi-material layup, the thermo-elastic behaviour of the LE needs to be considered in the CFRP layup selection and the rib attachment design. The integration of erosion protection and electro-thermal WIPS as integral parts of the LE lead to a multi-material structure with different physical properties, including the coefficient of thermal expansion (CTE), in the thickness direction. With the wide range of temperatures potentially experienced by a composite aircraft component, this leads to significant thermal deformations affecting the flight shape and shape of a loose replacement LE alike, potentially disturbing aerodynamic performance and hindering interchange.

The thermal-induced deformations are accompanied by composite-specific phenomena. Some, like warpage or the irreversible part of the spring-in phenomenon, result from the production process conditions and the part design itself. Compensation strategies and corresponding simulation frameworks are in general available [30] and are included in the design of a composite part to reach a certain target geometry. The state-of-the-art aircraft structural design of LE attachments fits the application of multi-material, functionally integrated structures poorly nonetheless. Through the presence of a multitude of fixed bearings in spanwise direction, each running along a LE rib from the tip of the profile up to the joint of LE and wing box, a complex deformation will be present between those bearings under aerodynamic and thermal loads, leading to local waviness between the LE ribs. The attachment concept has to take care of this.

3.2. Mechanical wing cover joint

A mechanical connection is made at the interface between the LE and the upper cover. The joint between LE and wing upper cover is highly driven by the aerodynamic requirements, since conventional designs rely highly on fasteners through the outer surface, creating 3d disturbances. The design choice also determines the possibility of LE interchange. The access to the inside of the LE segment provided by the Krueger flap enables the positioning of the fastener elements on the inside of the structure. To support this, the wing cover has an integrated vertical assembly element on the inside, called the LE stringer. The wing cover continues over the LE stringer with a small overhang. The LE has a matching integrated L-angle. Figure 5 shows these features in a section of the LE joint with the upper cover.

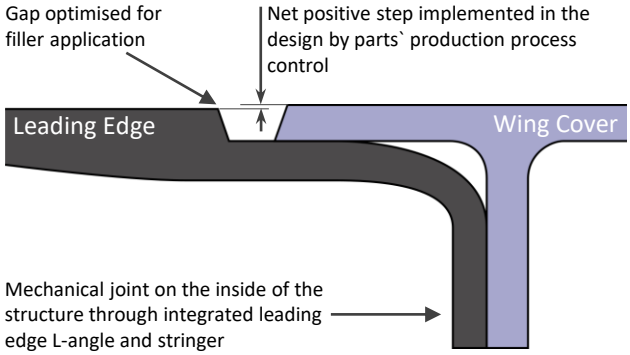

Figure 5: Detailed view of the upper cover joint arrangement.

To further enhance the ability for a quick interchange of damaged LEs, the fasteners through L-angle and LE stringer are positioned in two eccentric bushings to enable a form fit through predrilled holes protected by permanently installed bushings in the holes as shown in Fig. 6.

With this approach, no alterations to a spare part have to be made in contrast to the state-of-the-art, where time-consuming transfer of hole patterns would be necessary. The second advantage of the eccentric bushings is their ability to provide a means of fine adjustment to the assembly: Through a defined relative rotation of the bushings, a purely vertical relative movement of the LE can be induced to establish a safe contact of the upper cover overlap and the LE landing to facilitate the compliant step height through the selection of the part's production processes.

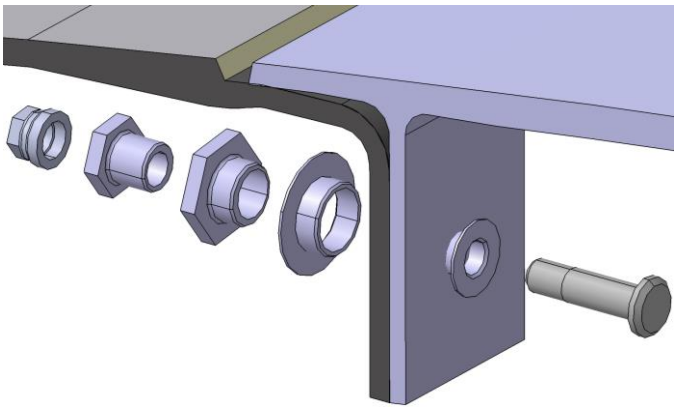

Figure 6: Detailed view of the fastener and eccentric bushings at the mechanical joint inside the structure.

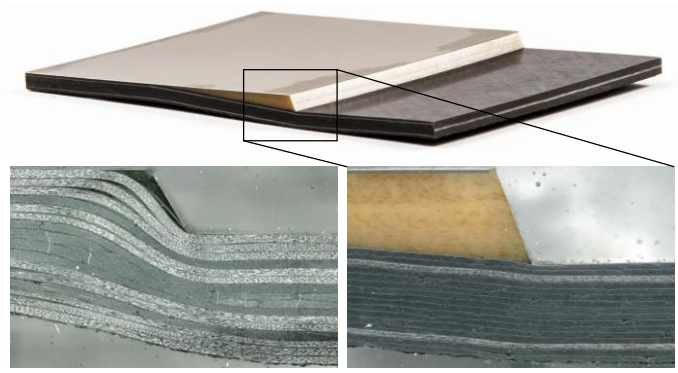

Figure 7: Improvements in integrated landing design: 100 mm wide test specimen of an integrated landing (top), section of a laminate with resin-filled edge prone to cracking (lower left, resin zone visibly in dark), and improved laminate detail at the edge with GFRP wedge and steel on the surface (lower right).

3.3. Laminar wing cover interface

In addition to the avoidance of fastener heads from the mechanical joint, the interface has also to consider the aerodynamic NLF allowables for FFS and BFS as presented in Section 2.2. Compliance with the step height requirement is ensured by the form fit of both LE and wing cover overhang and by the use of fitted fastener elements through L-angle and LE stringer that prevent any change in the step. The step height control itself is achieved by a suitable selection of production processes: The upper cover overhang thickness is controlled by a closed mould and the recess for the upper cover overhang on the LE is formed directly by an open mould. Thus, material thickness variations typical to composite components produced from prepregs in open mould processes have no influence on the joint's step height. The option to use an individually applied filler between the components to achieve a minimum step between the wing cover and LE is dismissed, for no alterations to a spare part are allowed in case of a necessary replacement.

Inside the structure, the LE forms a landing. The landing is defined as the horizontal support where the wing cover overhang rests on the LE skin segment running under the wing cover. This landing, as well as the L-angle of the LE where the mechanical connection is made, is directly formed by the continuous fibres of the LE skin. For a structural component, sharp edges and changes in the direction of fibres should be avoided, as they may result in damage to fibres in the production process and out-of-plane stresses under load. However, such edges can be found in structures nonetheless. The application of a ramp or a sufficiently large radius at the edge of the recess in the LE is no option for an NLF application. A radius would lead to an undefined run out with an infinitesimal low thickness of a gap filler material. A sharp edge in contrast would provide a controlled environment for filling, would however without other remedial measures lead to above mentioned possible disadvantageous structural effects. The edge itself would, since carbon fibres will not fill the edge of a mould cavity, be filled with the matrix resin of the composite used. Resin-rich areas are more brittle and could get lost over time in operation, leaving an undefined, larger gap or creating a gap in front of the filler.

To mitigate the negative impact on structural performance and provide the defined edge at the interface, a wedge inlay is introduced. With approximately 5 mm of constant thickness directly at the gap and a taper ratio of 1:10, it allows for a smooth redirection of structural fibres and WIPS layers towards the inside of the structure. Figure 7 shows microsections of a recess with and without wedge inlay and a fully integrated landing specimen. GFRP is selected as wedge material since it can be integrated into the composite production process seamlessly. The steel foil erosion protection ends right at the gap, too. The recess in the LE itself is designed to shift the target step height between LE and wing upper cover to 0.2 mm, to avoid the closeness of a target zero step height to the more sensitive BFS tolerance. The gap wall is defined with a 70° angle.

3.4. Rib attachment

The design of the rib attachment addresses the requirement to avoid fastener heads on the surface and serves the needs of the multi-material layup. In conventional design, fastener heads are present on the outer surface where a LE is bolted to a forward wing rib flange. The multi-material design of the LE skin poses another important boundary condition: Caused by the asymmetric application of the erosion shielding's steel foil on the LE's surface and the mismatch of the CTE of CFRP, steel and WIPS structure, variations in temperature lead to shape changes of the LE. High temperatures in the fibre composite production and temperatures varying over a wide range in aircraft operation demand compensation of the associated deformations in the LE's production process as well as a tailored attachment to deliver the shape necessary for sustained laminar flow under cruise flight conditions.

To address both fastener heads on the surface and thermoelastic deformations, the attachment concept removes any direct connections between forward wing ribs and upper LE skin. Thus, first of all, fastener heads are removed from the surface. Second, local waviness between ribs is prevented and a fit problem is resolved: Whatever a detailed design of a direct attachment between ribs and LE skin might be, the multi-material structure would have a different shape at different assembly temperatures. This would require adaptions or the use of excessive force if LE exchange is necessary. At the same time, it

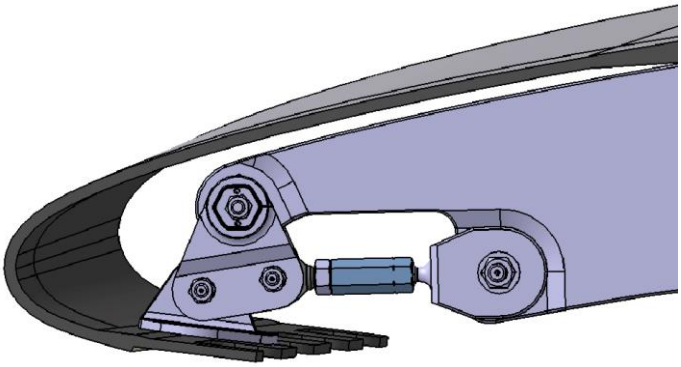

Figure 8: The rib attachment in the GBD assembly.

would be arguably hard to impossible to compensate the production tool of a multi-material composite structure as used within this project if a conventional attachment would have been used. Local deformations between ribs would have to be compensated in the tool surface and tailored to achieve a nominal profile shape in cruise flight under aerodynamic and thermal loads. The LE would have to be produced with pre-formed bulges between the ribs that achieve their smooth, nominal shape in cruise flight. This shape would be very complicated to simulate for compensation and its producibility is highly questionable. Local 3d plastic pre-deformation of the steel foil would be necessary as well as an equally shaped curing mould, where both parts would have to achieve a tight fit when the preform is placed in the mould.

The new attachment concept translates this to a global deformation challenge only. The LE in this concept is only supported at the joint to the upper wing cover and by a pendulum strut-like connection between the ribs and the lower end of the LE where the Krueger flap connects to the LE when retracted (Fig. 8). This allows for a ”free” and controlled deformation of the LE surface under thermal and mechanical loads over its chordwise direction and span. This global deformation can be predicted and tailored to cruise conditions. Deviations in non-cruise flight can be tolerated, for the associated free flow conditions oppose effective support of the laminar boundary layer anyway.

The pendulum strut is designed to support the LE profile in vertical and chordwise direction through the connection to two lugs at each rib. The strut in chordwise direction allows for adjustment to tolerances through a turnbuckle. In the vertical direction, a combination of an eccentric bolt and an eccentric bushing is introduced to allow for tolerance compensation. This capability is discrete, for the bolt and bushing are secured by form fit in their rotational degree of freedom, with 12 positions possible. Each connection at the rib and LE uses a spherical bearing to allow for tolerances and small movement out of the rib plane. The selection of the eccentric bolt/bushing combination in the vertical link is a special design only necessary for the outer wing and not a necessity of the concept. The LE profile is becoming so thin, that a conventional turnbuckle design is no more applicable here. Other design solutions are possible.

The fittings on the LEs are placed on the landing where the closed Kruger flap is located. Fasteners through the composite structure are thus placed where they are covered by the Krueger flap in flight. The LE surface on the lower side is thus kept free of disturbances up to the interface of LE and Krueger flap.

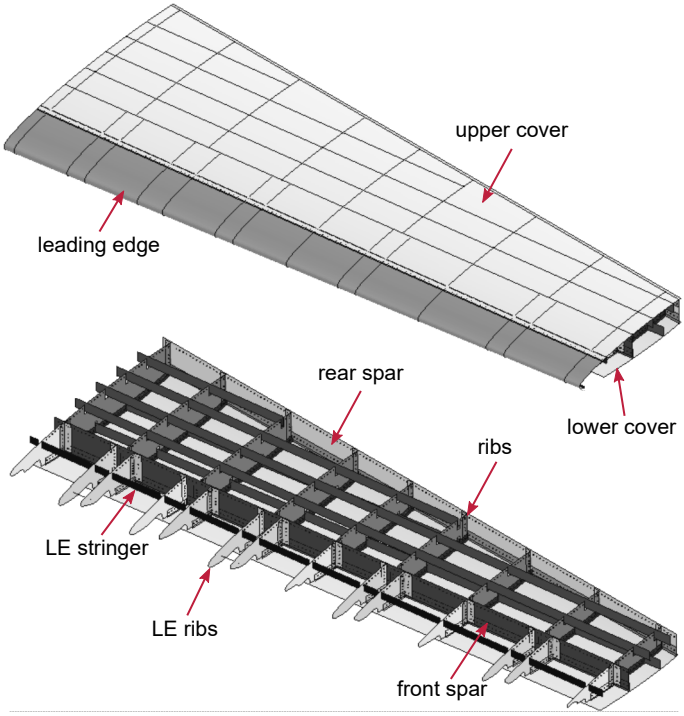

Figure 9: Detailed structural model of the 4.5 m long outer section of the NLF wing investigated in the FEA.

4. Numerical design verification

The multi-material laminar LE design presented in Section 3 is verified numerically by means of finite element analysis (FEA) with regard to the NLF requirements listed in Table 1. Since laminar flow is very sensitive to surface discontinuities in terms of steps and gaps, special attention is paid to the interface between the LE and the upper wing cover. Interface steps are only evaluated at the NLF design use case under cruise flight conditions. NLF conditions are for the purpose of this article not considered to be present outside of cruise flight. The structural model is a detailed design of a 4.5 m long outer wing section (cf. Fig. 1). The structural elements implemented in the model are shown in Fig. 9. The nominal wing shape is identical to the shape of the unloaded wing at assembly temperature, i.e. shape compensation for flight loads is not yet considered in the design process. Sizing and verification of all components, including forward wing ribs, is done using several manoeuvre load cases.

The LE laminate has a major influence on meeting the NLF requirements due to its asymmetrical layup driven by operational constraints, as described in Section 3.1. In particular, bending–twist coupling induced by different CTE and by 45° and −45° UD layers distorts the LE under operational loads. The LE distortions increase the upper cover joint’s step height and affect the NLF requirements. Therefore, optimising the

LE's CFRP base layup and stacking sequence can reduce bending–twist coupling, which is a prerequisite for maintaining laminar flow. In addition, the LE layup strongly affects assembly forces during LE interchange and fastener forces during flight.

A numerical study on the variation of the LE's CFRP base layup is conducted aiming to reduce bending–twist coupling induced by 45° and −45° UD layers, to improve the LE interchangeability by the reduction of assembly forces, and to reduce loads and fastener forces in critical load cases. Since the asymmetrical multi-material LE laminate is affected by changes in temperature, the effect of assembly temperature on step height and fastener forces is evaluated to assess the LE under changing operational conditions. The numerically verified multi-material LE design forms the basis for the realisation of a functional demonstrator.

4.1. High-fidelity FEA model

A precise prediction of the structure's loading and deformation under operational aspects requires a high-fidelity engineering model. This study uses the simulation software MSC Nastran to model the outer wing section shown in Fig. 9 with a section width of 4.5 m. The primary structural components of the wing box and LE are modelled in detail using 2D shell elements (CQUAD4, CTRIA3), whereas non-structural masses are modelled as concentrated mass elements (CONM2). The material parameters for composites are written in PCOMP cards. Stiffnesses of fastener elements (CFAST) are calculated using the Huth formulation [31]. The degrees of freedom provided by the flexible rib attachments are realised using rigid body elements (RBE2, RBE3).

Table 2 shows the load cases investigated. This paper aims to show that the presented LE design is able to fulfil the NLF requirements from Table 1. However, laminar flow is highly sensitive to upstream turbulences, and therefore, the laminar flow requirements are only investigated for the cruise load case. In particular, the step height at the interface between the LE and the upper wing cover is evaluated since this is the most critical area for laminar flow from the structural design point of view. The calculation of the step height is performed by evaluating the difference in node displacements on both sides of the wing cover interface relative to the local flow direction. The cruise load case applies aerodynamic loads as surface distributed pressure loads and thermal loads representing the temperature difference between assembly ($T_{\text{assembly}} = 23\,°\text{C}$) and altitude ($T_{\text{cruise}} = -56\,°\text{C}$).

Critical flight load cases are investigated to prove that the structure withstands ultimate flight loads. Therefore, static strength (Tsai-Wu failure theorem), stability (linear buckling analysis) and fastener loads (shear and axial loads) are evaluated. Two most critical load cases are identified limiting the flight envelope: a gust load case with a load factor of $n_z = 2.78$ and a manoeuvre load case with a load factor of $n_z = -1$. Referring to EASA's certification specification CS 25 [14], limit loads are multiplied by 1.5 to receive ultimate loads. Flight loads are applied as shear–moment–torsion (SMT) loads [32] introduced at the ribs inside the wing box.

In addition, investigations on LE interchangeability are performed, which is necessary e.g. after bird strike. In a best-case scenario, the removal of a damaged LE and installation of a replacement can be performed on an aircraft without the need to unload the wing via specialised racks at any airport worldwide under all climate conditions of the aircraft's operational envelope. The on-ground load cases investigate the LE interchangeability for a wing deflected by gravity and exposed to thermal loading. Initially, assembly in an air-conditioned shop floor at $T_{\text{assembly}} = 23\,°\text{C}$ is considered. Subsequently, assembly performed on an airfield at extreme ambient temperatures (−70 °C to 90 °C [13]) is investigated to assess the influence of operational aspects on NLF requirements.

4.2. Layup selection driven by operational requirements

Implementing a NLF LE is challenging since the interface between LE and upper wing cover can induce disturbances in the flow causing a laminar–turbulent transition. Narrow limits for step heights must be fulfilled to enable NLF. The asymmetric multi-material LE structure presented in Section 3.1, however, induces bending–twist coupling when subjected to structural and thermal loads, resulting in a shape change at the wing cover interface. Therefore, the layup of the LE laminate has a significant effect on satisfying the NLF requirements at the wing cover interface. This section describes the selection process of an advantageous layup for the LE's CFRP base structure by means of FEA under consideration of operational requirements.

A set of different LE layups is defined covering the reasonable design space considering general design rules for fibre-reinforced plastics. In particular, the layups are balanced, the minimum fibre amount in each of the four principle directions is 10%, and the maximum number of adjacent plies of the same orientation is three [33, 34]. Fibre angles are limited to [0°/45°/−45°/90°] due to manufacturing reasons. In this paper, a selection of the four most expressive layups is presented, shown in Table 3. These are a quasi-isotropic layup, a layup with maximum spanwise bending stiffness (0°-dominated), a layup with minimum spanwise bending stiffness (90°-dominated), and a shear laminate (±45°-dominated). Several more layups were investigated, but their results are in between the results of the aforementioned layups and do not show advantages compared to the presented layups.

The layups are evaluated with regard to aerodynamic step height, loads on fastener elements, assembly forces, bending–twist coupling, static strength, and stability. Figure 10 shows the step height at the interface between LE and wing cover for all laminates as a function of spanwise coordinate. The limits of the diagram describe the aerodynamic limits for laminar flow that are given in Table 1. The variation in step height is small for all laminates at medium span and increases at the segment edges caused by the fixed connection between end ribs and LE skin in the FE model. The step height is within the limits required for maintaining NLF.

Figure 11 shows the shear forces experienced by the fastener elements at the wing cover interface for all laminates in

Table 2: Load cases investigated.

Load case	Structural loads	Thermal loads	Investigated parameters
Cruise	$n_z = 1$ (surface pressure)	−56 °C	Laminar flow requirements (step height)
Critical gust	$n_z = 2.78$ (SMT loads)	−56 °C	Static strength, stability and fastener loads
Critical manoeuvre	$n_z = -1$ (SMT loads)	−56 °C	
On ground (hot/mid/cold)	Gravity	90 °C, 23 °C, −70 °C	LE interchangeability

Table 3: Different layups for the CFRP base structure of the multi-material LE. The LE part coordinate system is oriented with respect to the front spar of the wing box with the 0°-layer oriented in spanwise direction.

Description	Layup
quasi-isotropic	[St/WIPS/(45°/ 0°/−45°/90°)$_{2s}$]
0°-dominated	[St/WIPS/(0°$_3$/45°/ 0°$_2$/−45°/90°)$_s$]
90°-dominated	[St/WIPS/(90°$_3$/45°/90°$_2$/−45°/ 0°)$_s$]
±45°-dominated	[St/WIPS/(45°/−45°/90°/−45°/45°/−45°/45°/ 0°)$_s$]

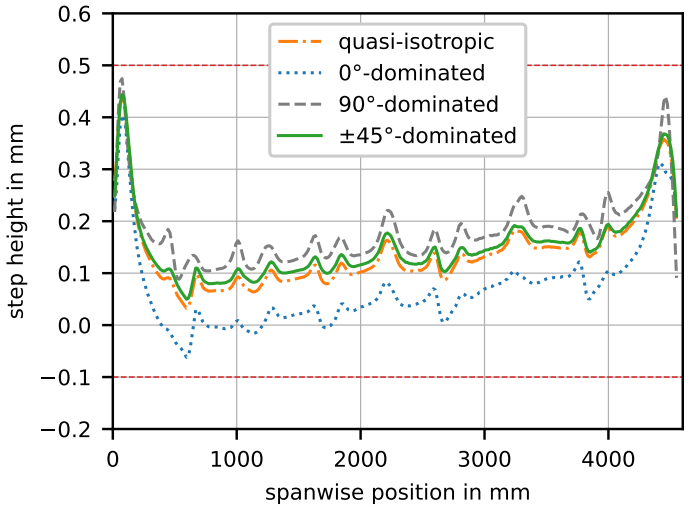

Figure 10: Step height in cruise for different LE layups. NLF allowables as red dotted lines.

Table 4: Coefficients of the ABD matrix for different CFRP base layups of the multi-material LE structure. D_{11} correlates with the bending stiffness of the laminate, whereas $B_{16}/B_{26}/B_{66}$ and D_{16}/D_{26} indicate the membrane–bending and bending–twist coupling.

Laminate	Coefficients			
	B_{16}, B_{26} in N	B_{66} in N	D_{11} in N mm	D_{16}, D_{26} in N mm
quasi-isotropic	$1.17 \cdot 10^0$	$-1.06 \cdot 10^4$	$7.22 \cdot 10^5$	$4.74 \cdot 10^4$
0°-dominated	$1.58 \cdot 10^0$	$-2.59 \cdot 10^4$	$1.17 \cdot 10^6$	$2.37 \cdot 10^4$
90°-dominated	$1.58 \cdot 10^0$	$-2.59 \cdot 10^4$	$3.40 \cdot 10^5$	$2.37 \cdot 10^4$
±45°-dominated	$1.71 \cdot 10^0$	$4.73 \cdot 10^3$	$5.14 \cdot 10^5$	$2.63 \cdot 10^3$

the most critical flight load cases. Axial fastener forces are determined as negligible compared to shear forces. The figure shows a strong dependence on the LE laminate and on the load case. The fastener forces increase with increasing bending stiffness in the 2.78 g gust load case, whereas the fastener forces are less dependent on the layup in the −1 g manoeuvre load case.

Assembly forces are estimated by replicating the wing on-ground bending curve during LE interchange. The LE is fixed at the inboard end, while a forced displacement is applied in the shear centre at the outboard end. It is assumed that the assembly forces correlate with the bending stiffness of the LE structure. The bending stiffness is calculated by using the compliant matrix of the LE laminate. Table 4 shows selected coefficients of the ABD matrix of all laminates. The D_{11} coefficient correlates with the spanwise bending stiffness and changes with a factor of about 3.5 between the different layups. However, the calculations show that the forces required to fit the LE on the deformed wing during LE interchange are small for all laminates.

The asymmetric multi-material LE laminate is prone to bending–twist coupling under structural and thermal loads. Figure 12 shows the free LE deformation due to thermal loads caused by different CTE in the multi-material LE laminate. With negative temperature differences, two effects are visible: upward bending in spanwise direction and an opening of the profile section. With positive temperature differences, the effects act in the opposite direction. Additionally, bending–twist coupling occurs that is dependent on the layup (number and position of 45° and −45° plies). Comparisons with Table 4 show a good correlation between the amount of bending–twist coupling and the magnitude of the coupling coefficients of the laminate's ABD-matrix (B_{16}, B_{26}, B_{66}, D_{16}, and D_{26}). By optimising the layup and stacking sequence, the coupling coefficients are reduced by one order of magnitude in the case of the ±45°-dominated laminate, resulting in an almost zero LE twist under thermal loads, as shown in Fig. 12 (d).

Further investigations indicate that both static strength and stability are of no concern for any layup investigated. No failure

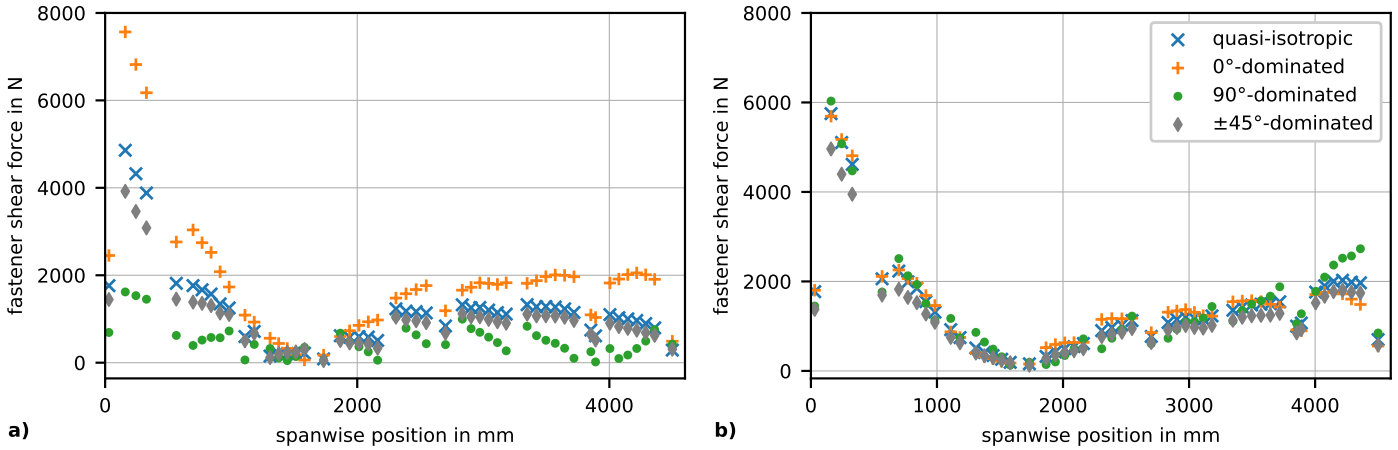

Figure 11: Shear forces at upper cover joint fasteners: (**a**) Gust load case with $n_z = 2.78$. (**b**) Manoeuvre load case with $n_z = -1$.

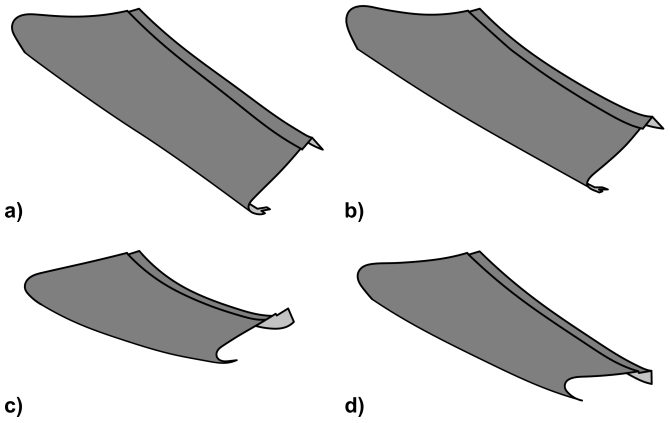

Figure 12: Thermal deformation of the LE at $T = -70\,°C$ for different layups: (**a**) quasi-isotropic, (**b**) 0°-dominated, (**c**) 90°-dominated, and (**d**) ±45°-dominated layup.

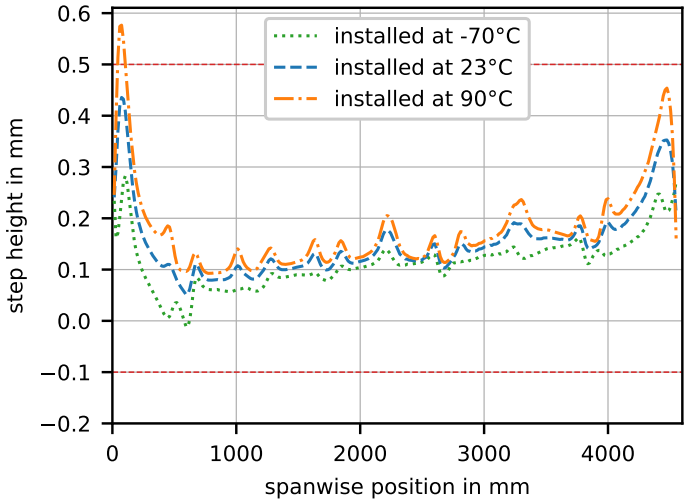

Figure 13: Step height at the wing cover interface in cruise for different LE assembly temperatures. NLF allowables as red dotted lines.

at ultimate load occurs in either the 2.78 g gust load case or the -1 g manoeuvre load case.

Based on the numerical results presented in this section, the ±45°-dominated layup is most advantageous for the multi-material NLF LE. Compared to all other investigated layups, the ±45°-dominated layup provides the best trade-off in terms of step height, fastener forces, assembly forces, and bending–twist coupling. Therefore, the ±45°-dominated layup is selected for implementation in the GBD and for the following numerical design verification.

4.3. Simulation-based design verification considering operational aspects

The design of the NLF-compliant LE is verified under additional consideration of operational aspects. The operational aspects are related to the interchangeability of the LE for an aircraft parking on an airfield at extreme ambient temperatures and free cantilevered wings. The effect of a variable assembly temperature on the NLF requirements (step height) and fastener forces is evaluated since thermal loads have a significant influence on the deformation of the asymmetric multi-material LE structure. The numerical model used for the design verification is the detailed structural model shown in Fig. 9 using the ±45°-dominated layup selected in the previous subsection for the multi-material LE structure.

Figure 13 shows the step height at the wing cover interface in cruise for a LE assembled at $T_{\text{assembly}} = -70\,°C$, 23 °C and 90 °C. The step height increases with increasing temperature difference between assembly and cruise ($T_{\text{cruise}} = -56\,°C$). However, the difference is small at medium span but increases at the segment edges.

A variation in assembly temperature also affects the loads acting on the fasteners at the mechanical joint between the LE and upper wing cover. Figure 14 shows that maximum shear forces that have to be considered for the dimensioning of the fastener elements are strongly influenced by the assembly temperature. The effect of the assembly temperature is opposite for the 2.78 g gust load case and the -1 g manoeuvre load case, since reduced assembly temperatures increase the fastener loads on an upwards bending wing, whereas enhanced assembly temperatures increase the fastener loads on a downwards bending

wing. The dependence of the fastener forces from the temperature difference is mainly driven by the different CTE in the single layers of the multi-material LE laminate.

The evaluation of static strength and stability reveals that all structural elements implemented in the detailed model of the outer wing section can bear the loads even in the worst combination of assembly temperature and flight loads. Moreover, it was shown that the NLF requirements, especially in terms of step height, are met for all investigated cases in cruise flight. Therefore, the presented design of a NLF-compliant multi-material LE structure in combination with the detailed wing box design and the flexible rib attachment proves to be suitable for realising a functional demonstrator.

5. Experimental validation

In the test-based validation, the interchangeability of the LE is to be demonstrated and the resulting step heights between LE and wing upper cover are assessed in the neutral, on-ground, and cruise deformation states of the wing. A GBD wing section and test rig for its deformation are designed for this purpose. The test rig and overall GBD design are summed up in this article. A more detailed account of the test rig optimisation process is publicly available [35]. Step height measurements on the demonstrator are made using a 3d optical measurement system and are subsequently analysed as discrete steps at automatically generated LE surface sections.

5.1. Test rig design and test article production

The GBD structure is designed to support the focus on the LE attachment through its design. It consists of a 2.3 m wing section connected to a test rig with electro-mechanical actuators to facilitate the deformation of the GBD. However, the wing section does not include a lower wing cover or a rear spar. As the demonstrator is intended to be deformed, those additional stiffening elements are deemed unnecessary and even disadvantageous for reaching the demonstration goals, because their use would have resulted in far larger deformation forces. Other than the LE with its attachment elements and wing upper cover, all structural components are not sized for aircraft operational loads. They are designed to support the function of the demonstrator. Figure 15 provides an overview of the test rig and GBD main components.

In detail, the demonstrator wing section consists of a CFRP wing upper cover, five CFRP box ribs and a front spar as well as eight machined aluminium LE ribs in addition to the LE. Six of the LE ribs support the floating LE attachment concept with struts, while both ribs at the end of the demonstrator have flanges to support an attachment with bolts through the outer surface of the LE. The underlying laminar wing concept with LE segments wider than 4 m permits turbulent joints between adjacent LE segments. This is adopted to the reduced span of 2.3 m on the demonstrator. The wing cover production is described in [36]. Also designed for NLF, it provides a surface with low waviness and without fastener heads on the outer surface. This is achieved by the integration of stringers, ribcaps and sparcaps.

The ribs, front spar and LE ribs are kept simple with regard to geometry and production. The strength of LE, wing cover and LE ribs is verified in the global FE model detailed in Section 4. The strength of the individual components of the rib attachments (see Fig. 8) is verified in separate detailed FE models using the nodal reaction forces of the RBEs used to represent them in the global FE model. The layup of box ribs and front spar is derived as part of the test rig optimisation process. The optimisation goal of the test rig optimisation process [35] is to minimise the deviation between surface deformation of the demonstrator achieved by the test rig and the cruise flight deformation target shape of the wing as achieved in the FE simulation of the outer wing (Section 4). The strength of all composite components of the demonstrator is assessed as an additional constraint (Tsai-Wu criterion) of the optimisation, including wing cover and LE already verified using the manoeuvre load cases in the wing FE model. Actuator positions, elongations and direction as well as rib and front spar thickness and their layup are parameters of the optimisation process. The demonstrator components are represented in an FE model, with a Python script iterating the parameters using the Mixed-Integer-Distributed-Ant-Colony-Optimization (MIDACO) algorithm [37]. In a series of optimisation runs, the number of actuators was set to six, which are placed vertically under the middle rib, two vertically under the outer rib, one vertically and one slanted under the front spar, with the latter to compensate for rigid-body rotation caused by the wing taper relative to the fixed bearing at the innermost rib. The bearing is free to rotate. The final test stand uses electro-mechanical actuators capable of applying 5 kN each, placed on a machine bed.

The composite ribs and spar of the box section were manufactured in-house using Hexcel M21 T700 prepreg material in a vacuum bag autoclave process. The box section of the demonstration structure is assembled using an adaptable, actively actuated test rig to compensate for the flexibility of the wing upper cover. Ribs and spars are placed in a rigid jig for the assembly process. The quality of the wing cover surface is checked with a GOM ATOS 3d scanning device during assembly and corrected using the actuators if needed [38]. The LE ribs use the wing cover LE stringer and predrilled holes for the LE assembly as a reference for installation.

The development of the LE production process was given special care, especially with respect to the integrated landing and GFRP wedge inlay. Suitable production parameters for the wedge are determined in an independent study [39]. The GFRP wedges for the LEs are stacked by hand to their wedge shape and then the tool-facing portion of the wedge is trimmed with a robot-mounted ultrasonic blade. The wedge is placed in the curing mould on top of the surface-treated erosion shield steel foil. The surface treatment of the steel foil is made according to [40]. The curing mould is three-parted, with the L-angle section and the Krueger landing portion removable from the main tool to address the undercuts and enable demoulding. The layup of the structural CFRP layers and the WIPS are preformed on a separate preforming tool and transferred to the curing mould with a dedicated jig. The curing mould is vacuum bagged and

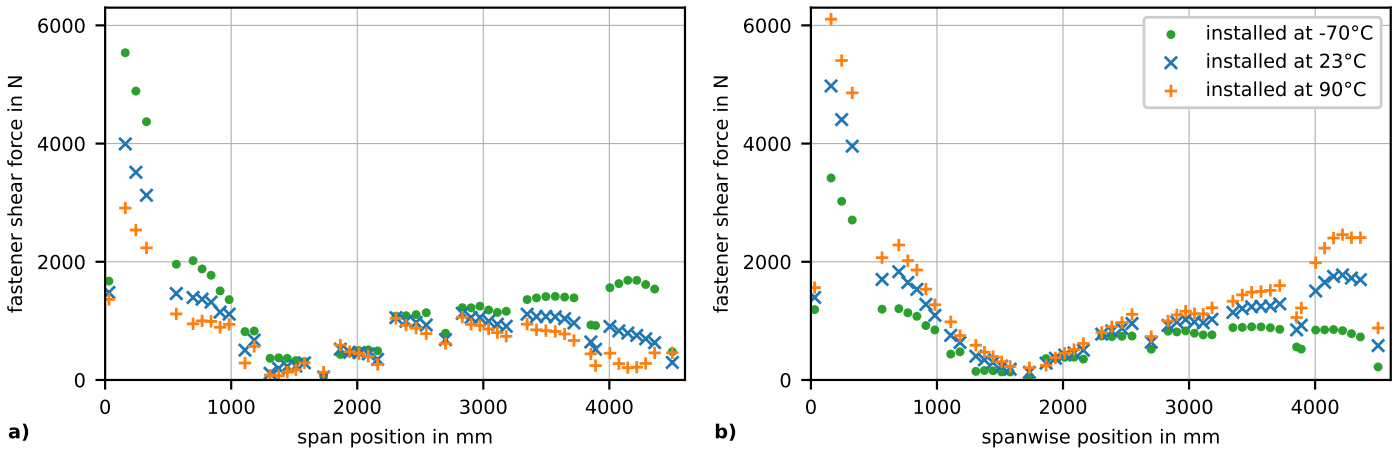

Figure 14: Shear forces at upper cover joint fasteners for different leading edge assembly temperatures: (**a**) Gust load case with $n_z = 2.78$. (**b**) Manoeuvre load case with $n_z = -1$.

Figure 15: Test rig and ground-based demonstrator setup.

the LE is cured in an autoclave process. A detailed account on the development of the LE production process is given in [41]. The GBD LE is compensated for spring-in at the L-angle and the profile and is in a pragmatic approach also considering thermal expansion of the components. The spanwise effects of the different CTEs of the structure's constituents are not considered in the compensation to not overcomplicate tooling design and manufacturing. The LE thus shows a global deformation as a result of the temperature difference $\Delta T = 159\,°C$ between the composite processing temperature and the installation test temperature. This deformation is present in all deformation states, including cruise, since no thermal loads are applied in the GBD tests.

5.2. Test procedure and assessment method

Two LEs are available for installation, LE2 and LE3. The LE number, installation state ("neutral" n or "on-ground" g) and deformation state measured ("neutral" n, "on-ground" g or "cruise" c) are subsequently given to designate a data set. The first number in the designation indicates the instance of the installation with the given LE in the given installation state, 1 or 2. In this case, 2 means this is the second data set with the exact same installation parameters as the set designated with 1 using the same LE installed in the same GBD deformation state. Four installations of a LE were made, three in the "neutral" deformation state (LE3n, LE3n_rep, LE2n) of the GBD and one in the "on-ground" state (LE2g). In all installations, all three deformation states of the GBD are used as measurement positions. Thus, 12 surface measurements are made (see Table 5). The installation states are selected to check the reproducibility of

the manual installation, compare differences between both used LEs and compare the operationally relevant installation in the on-ground state to the neutral state.

The LE installation procedure is made up of five steps. The LE is (1) fitted to the wing box loosely supported by the end ribs, where bolts are placed to prevent the LE from dropping away. Eccentric bushings and fasteners are placed at the joint to the upper cover (2). Fasteners are tightened to a degree where axial movement is prevented (Fig. 16, right). Then, bolts at the rib attachments are placed (3) (see Fig. 16, left). Beginning in the middle of the LE's L-angle, the eccentric bushings are subsequently adjusted and the respective fasteners are tightened to secure the connection when safe contact between LE landing and wing cover overhang is achieved (4). The contact between both parts, conceptually delivering the desired step height, is checked in the installation process using a light gap method. On the LE stringer radius of the wing cover, an LED light band is placed along the span of the GBD in a void between LE and wing cover. The light can be seen on the wing surface looking at the gap between LE and wing cover. If contact between both parts in vertical direction is achieved by manipulation of the eccentric bushings, the light is no longer visible, giving simple optical feedback. The installation is concluded by tightening the bolt at the end ribs (5) only placed to secure the LE in step 1.

The measurement of the surface is done with a GOM Atos 3d optical measurement system. Spanwise sections of the surface are exported and used in a Python script that automatically identifies the surface points of the wing cover and LE and constructs a point at the edge of the wing cover in the respective section at which the step height is measured as the distance between the fitted curves of the LE and wing cover surface points. The step height is measured normal to the LE curve to represent the projected step height of the slightly sloped flank of the gap the airflow from the LE surface would pass. The measurements thus reference a virtual airflow over the gap tangent to the measured LE surface. A detailed account of the automated step estimation tool is given in [42].

5.3. Test results

The results of the test made with the GBD are categorised as results in step heights achieved in the installation of both LEs and a more refined comparison of the differences observed between installations as a means to assess if interchangeability is achieved.

5.3.1. Step heights

Figure 17 shows the step height over GBD spanwise coordinate for LE no. 3 installed in the neutral position and measured in all three deformation cases. The graph shows the rib positions as vertical dotted lines. Clearly visible boundary effects at the start and beginning of the LE are visible, comparable to the effects visible in the simulations. The graphs show a global tendency of decreasing step height over the span. Disregarding the boundary effects all measured steps are located in a corridor of about 0.2 mm. At the last section of the LE to the upper cover joint between rib no. 6 and the end rib, the step height slightly undercuts the NLF allowable of a 0.1 mm BFS. With a local maximum at the rib no. 5 at spanwise coordinate approx. 1600 mm, a pronounced anomaly can be identified. Deviations between deformation states are small. The diagram for installation 1LE3n is shown exemplarily. The plots for all four installations are very similar. For comparison, Fig. 18 can be referenced.

Figure 18 shows the step height over the spanwise coordinate in the neutral deformation state of each LE deformation. With the exception of LE2gn, the plots show the step in the state of the LE's assembly prior to any deformation. In general, the graph shows a small deviation between the steps for different installations, with the same distinct features. LE no. 2 shows in the innermost area of the GBD significantly larger step heights as are present in both installations of LE no. 3.

The distinct features in the plots can be explained by existing deviations of the build status to a nominal geometry. From [38], it is known the wing box has, as was expected by the wing cover used, not the nominal CAD shape. This is confirmed by optical measurements using the GOM Atos system. In addition to the box shape as-is, the LE end ribs show a tendency of an increasing deviation in their angle compared to the wing cover surface, leading to a light torsion of the LE towards the outermost rib, with the profile pointing more downward than at the inner endrib. Such a deviation would lead to the LE surface tangent in the affected sections pointing increasingly upward, leading to the interpretation of smaller step heights in the chosen assessment methodology. The pronounced anomaly at the approximate GBD span coordinate of 1600 mm can be interpreted by a similar mechanism. The LE ribs at this position have been identified to be located higher relative to the neighbouring ribs. This lifts the attachment point between rib and LE, leading to a relative rotation of the LE profile with respect to the upper cover joint. The LE tangent is pointing lower relative to the neighbouring areas of the joint. The assessment method would deliver (relatively) higher step heights. Local effects from wing cover thickness deviations can be ruled out.

The seemingly extended boundary effect of LE2 visible in Fig. 18 can be traced to fastener holes out of tolerance. The capacity of the eccentric bushings to compensate for hole deviations of 0.5 mm in each part is exceeded. In the measured state of the GBD, the eccentric bushings are adjusted to their maximum compensatory capacity, however, fail to establish contact between LE and wing upper cover overhang in the affected fastener positions, evident by the still present light gap in the assembly process.

Figure 19 shows the global surface deformation of the GBD measurement of installation LE3nn compared to the CAD surface as a best fit over the coloured area. Note that measurements based on a best fit are always highly dependent on the surfaces selected for the fitting and local measurements contain components from the global positioning that minimises deviations for the whole surface. As expected a characteristic global deformation of the LE can be observed as a result of the production process, with a minimum of −2.47 mm (measured surface below nominal surface) in this reference system. The fact

Table 5: Test overview.

Scope of tests	Data set name	Installation state	Measurement state
Interchangeability	LE3nn, LE3nn_rep, LE2nn	neutral	neutral
Deformation reversibility	LE3ng, LE3ng_rep, LE2ng	neutral	ground
NLF compliance	LE3nc, LE3nc_rep, LE2nc	neutral	cruise
Operational interchangeability	LE2gg	ground	ground
Deformation reversibility	LE2gn	ground	neutral
NLF compliance	LE2gc	ground	cruise

LE_i_j_k_rep: i = specimen number, j = installation state, k = measurement state, rep = repeated

Figure 16: LE rib attachment (left) and joint to the upper cover with eccentric bushings (right) on the GBD.

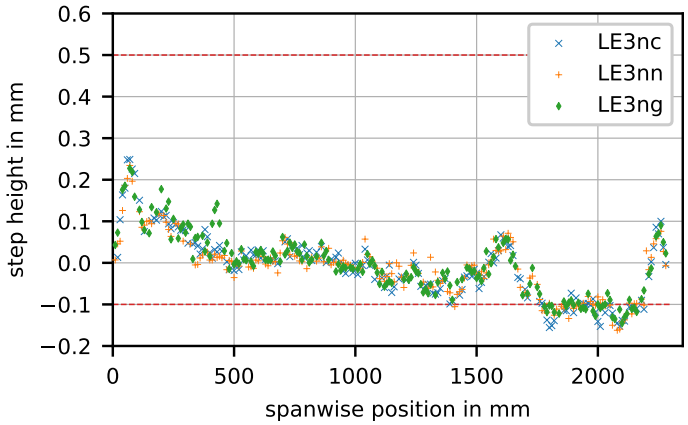

Figure 17: Step heights for all deformation states for test series LE3. NLF allowables as red dotted lines.

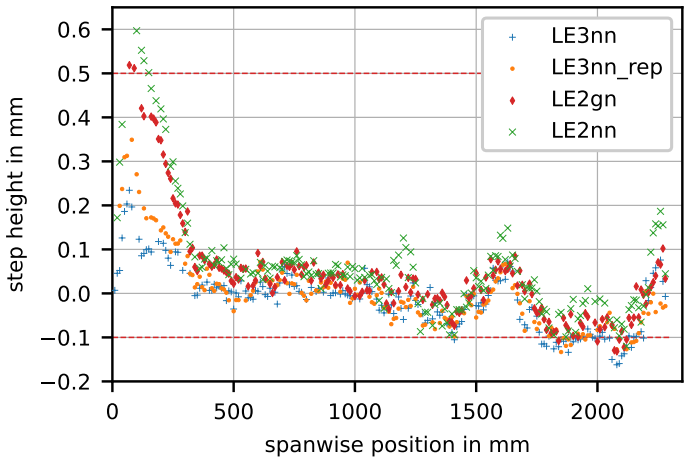

Figure 18: Step heights for all installations in the neutral position. NLF allowables as red dotted lines.

that the determined step heights at the interface of LE and wing cover are in a tight corridor mostly within the NLF threshold, proves the concept allows for a global deformation of the LE skin while retaining a rigid joint at the locations with higher tolerance requirements. With respect to profile tolerances, Heinrich and Kruse [43] have shown for an NLF wing that spring-in induced surface deformations and aerodynamic loads can compensate for each other. The process-induced deformations of the LE through the multi-material LE are not directly comparable through the effects of the different CTEs throughout the structure, however, the direction of the global deformation of the LE and the aerodynamic loads have equally opposing directions of action in this case. A partial mutual elimination seems possible as well as the 3d compensation of process-induced deformations to a defined degree.

5.3.2. Interchangeability

To assess the repeatability of the installation as a measure to prove interchangeability, Fig. 20 shows the mean value of the spanwise differences between the step heights measured in

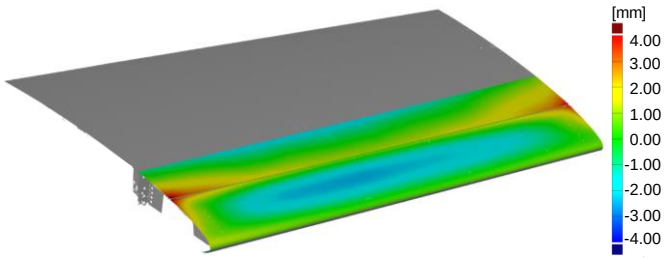

Figure 19: Global best-fit comparison of surface measurement to CAD for LE3nn.

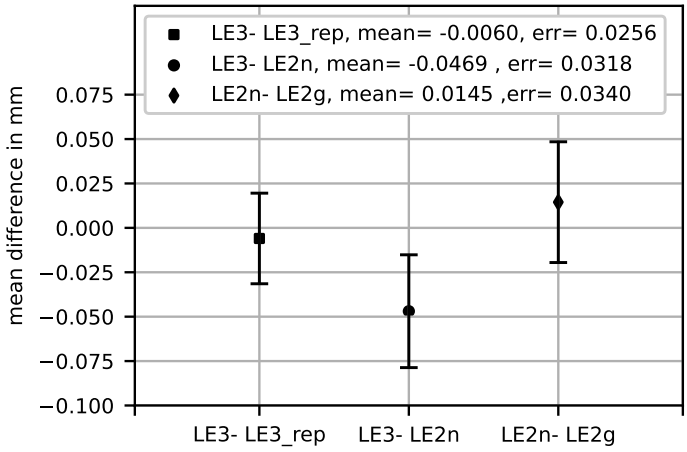

Figure 20: Mean differences of step heights between different installations.

the installation states between different installations. Only measurements between 350 mm and 2140 mm are used in this comparison. In this section, the out-of-tolerance holes at the joint of LE2 are neglected to establish comparable conditions for the comparison of the installation runs. The first difference LE3-LE3_rep, shows the repeatability for the same LE in the same installation state. LE3-LE2 shows the mean difference between the two LEs used in the same installation state and LE2n-LE2g enables a comparison between the same LE for installation in neutral and on-ground state. The smallest mean difference is achieved for a repeated installation of the same LE (LE3) with −0.0059 mm. The largest mean difference is measured between both installation states of LE2. However, all mean differences are small with absolute values below 0.05 mm.

Thus, the results show a high degree of repeatability of the manual installation process. The achievable installation accuracy seems higher than the manufacturing-dependent variation introduced through the use of different parts. The results shown in Fig. 17–20 have shown both repeatability of the installation of a LE using the developed attachment concept on the same LE, the general interchangeability with a replacement LE and the feasibility of both under on-ground deformation of the GBD wing section.

The interchange of two LEs, including de-installation of all bolts and fasteners, LE removal, preliminary fitting of the replacement LE and subsequent adjustment of the eccentric bushings, was done by two engineers in 3 hours and 43 minutes. With a full LE span roughly twice the width of the GBD and assuming a linear scaling of interchange time with increasing width, the goal of a full LE segment interchange in one night shift is achievable.

6. Conclusion and outlook

A multi-material LE and attachment concept for a NLF wing have been developed. The interface of the LE and wing cover has been investigated in detail. To simplify the assessment, the step height between LE and wing cover was assessed over a gap between both parts. *In praxi*, the gap would be closed with an elastomer filler. However, for filled gaps/ramps, no simple means of assessment exists yet. The assessment as a step was chosen as an available and conservative method. The LE attachment concept has demonstrated its interchangeability under operational boundary conditions. The repeatability of installation results with respect to step height at the interface between LE and wing cover is high for the same LE as well as for a replacement LE. Interchange is also possible under wing deformation and was achieved for the GBD LE in 3 hours and 43 minutes. The use of the eccentric bushings on the LE to upper cover joint delivers similar local spanwise step height results for different installations. The magnitude of step height variation between installations is far lower than the effects observable from wing box assembly deviations. The inclusion of operational aspects in the design of a NLF LE has therefore been demonstrated not to be in opposition to the practical application of the NLF concept in general.

The method of allowing the multi-material LE skin to deform globally and securing the relative position of LE and wing cover at their interface has been proven to be robust. Despite the production-induced, significant thermo-elastic deformations of the GBD LE, the step height at the interface is kept in a tight band of variation and fulfils the NLF requirements in a vast majority of the GBD's span.

Both simulation and test show the thermal aspects being more influential on the step height for a multi-material structure than wing bending. Thermo-elastic behaviour of multi-material structures has therefore a high importance for laminar flow research. Global part compensation for cruise flight appears to be necessary. In the next step, the global profile shape should be investigated in a coupled aero-structural simulation. Even when the part would be compensated for a nominal shape in cruise conditions, the global shape would deviate at other temperatures. Since the investigation in this paper shows a relatively small variation of step height over the span, this can be tailored to a certain degree together with the nominal geometry target step height to enable a trade-off between cruise shape and the shape at other flight conditions, including extreme cases for takeoff and landing. To shift the interface step height further towards the middle of the NLF tolerance band, the as-built step height can be adapted accordingly.

As a logical next step, the investigations made within this paper should be expanded to cyclic loading of the GBD. The influence of thermo-elastic deformations of the multi-material structure on a LE interface gap filler shape at different thermal conditions should also be considered. Aerodynamic per-

formance and manoeuvre characteristics of wings with multi-material LEs as presented within this article should be investigated at different temperatures across the operational envelope to assess the impact of thermo-elastic deformations outside of NLF-related considerations, too. With LE interchange scenarios now considered in NLF wing research, the application of laminar flow technology to large passenger aircraft is one step closer.

Declaration of competing interest

The authors declare that they have no known competing financial interests or personal relationships that could have appeared to influence the work reported in this paper.

CRediT author statement

Olaf Steffen: Conceptualization, Validation, Formal Analysis, Investigation, Data Curation, Writing – Original Draft, Writing – Review & Editing, Visualization, Supervision, Project Administration. **Patrick Meyer**: Conceptualization, Methodology, Software, Validation, Formal Analysis, Investigation, Data Curation, Writing – Original Draft, Writing – Review & Editing, Visualization. **Christian Hühne**: Validation, Resources, Writing – Review & Editing, Supervision, Funding acquisition.

Acknowledgements

This research was funded as part of the Clean Sky 2 programme under the grant agreements CS2-AIR-GAM-2014-2015-01 through CS2-AIR-GAM-2020-2021-01.

References

[1] R. D. Joslin, Aircraft laminar flow control, Annu. Rev. Fluid Mech. 30 (1) (1998) 1–29. doi:10.1146/annurev.fluid.30.1.1.
[2] G. Schrauf, Status and perspectives of laminar flow, Aeronaut. J. 109 (1102) (2005) 639–644. doi:10.1017/S000192400000097X.
[3] H. Hansen, B. Schlipf, Laminarität für zukünftige verkehrsflugzeuge: Überblick, anforderungen und status, Presented at Wissenschaftstag Braunschweig 2015, Braunschweig, Germany (7 October 2015).
[4] B. H. Carmichael, Surface Waviness Criteria for Swept and Unswept Laminar Suction Wings, Norair, a division of Northrop Corporation, 1959.
[5] J. P. Nenni, G. L. Gluyas, Aerodynamic design and analysis of an lfc surface, Astronaut. Aeronaut. 4 (7) (1966) 52–57.
[6] K. S. G. Krishnan, O. Bertram, O. Seibel, Review of hybrid laminar flow control systems, Prog. Aerosp. Sci. 93 (2017) 24–52. doi:10.1016/j.paerosci.2017.05.005.
[7] H. Hansen, Laminar flow technology – the airbus view, in: 27th Congress of the International Council of the Aeronautical Sciences, International Council of the Aeronautical Sciences (ICAS), Stockholm, Sweden, 2010, pp. 453–461.
[8] M. Fujino, Design and development of the hondajet, J. Aircr. 42 (3) (2005) 755–764. doi:10.2514/1.12268.
[9] M. Kingsley-Jones, Farnborough: Aero secrets of boeing's new dreamliner, Available online: https://www.flightglobal.com/farnborough-aero-secrets-of-boeings-new-dreamliner/113955.article (accessed on 09 15 August 2023) (18 July 2014).
[10] J. König, T. Hellström, The clean sky "smart fixed wing aircraft integrated technology demonstrator": Technology targets and project status, in: 27th Congress of the International Council of the Aeronautical Sciences, International Council of the Aeronautical Sciences (ICAS), Stockholm, Sweden, 2010, pp. 5101–5110.
[11] E. Hörberg, T. Nyman, T. Hellström, M. Rudlund, J. Bohlin, R. Berg, Shape distortion analysis of a complex shaped wing skin section, in: 20th International Conference on Composite Materials (ICCM 2015), Aalborg University, Aalborg, Denmark, 2015, pp. 1–11.
[12] K. Wicke, M. Kruse, F. Linke, Mission and economic analysis of aircraft with natural laminar flow, in: 28th Congress of the International Council of the Aeronautical Sciences, International Council of the Aeronautical Sciences (ICAS), Stockholm, Sweden, 2012, pp. 389–402.
[13] I. Moir, A. G. Seabridge, Aircraft Systems: Mechanical, electrical, and avionics subsystems integration, 3rd Edition, John Wiley & Sons, Chichester, West Sussex, UK, 2008.
[14] European Union Aviation Safety Agency, Certification specifications and acceptable means of compliance for large aeroplanes (cs-25): Amendment 27 (2021).
[15] B. H. Carmichael, Summary of past experience in natural laminar flow and experimental program for resilient leading edge: Nasa cr-152276 (1979).
[16] Airbus Operations GmbH, Multi-optimierung und verifizierung von entwürfen durch performance tests und simulationen : Movable design, optimisation and airframe noise reduction : Förderprojekt im rahmen des luftfahrtforschungsprogramms lufo iv-4 des bmwi der bundesregierung : Schlussbericht zur veröffentlichung move.on (2016). doi:10.2314/GBV:874007445.
[17] B. J. Holmes, C. J. Obara, G. L. Martin, C. S. Domack, Manufacturing tolerances for natural laminar flow airframe surfaces, SAE Trans. 94 (4) (1985) 522–531. doi:10.4271/850863.
[18] C. J. Obara, B. J. Holmes, Roughness and waviness requirements for laminar flow surfaces: N88-14953 (1986).
[19] J. A. Franco Sumariva, S. J. Hein, Adaptive harmonic linearized navier-stokes equations used for boundary layer instability analysis in the presence of large streamwise gradients, in: 2018 AIAA Aerospace Sciences Meeting, American Institute of Aeronautics and Astronautics, Reston, Virginia, 2018. doi:10.2514/6.2018-1548.
[20] J. A. Franco Sumariva, S. J. Hein, E. Valero, On the influence of two-dimensional hump roughness on laminar–turbulent transition, Phys. Fluids 32 (3) (2020). doi:10.1063/1.5131577.
[21] O. Steffen, C. Uckert, E. Kappel, T. Bach, C. Hühne, A multi-material, multi-functional leading edge for the laminar flow wing, Presented at 27th SICOMP Conference on Manufacturing & Design of Composites, Linköping, Sweden (30-31 May 2016).
URL https://elib.dlr.de/107314/
[22] K. V. Pool, C. K. H. Dharan, I. Finnie, Erosive wear of composite materials, Wear 107 (1) (1986) 1–12. doi:10.1016/0043-1648(86)90043-8.
[23] D. A. Gorham, J. E. Field, The failure of composite materials under high-velocity liquid impact, J. Phys. D: Appl. Phys. 9 (10) (1976) 1529–1541. doi:10.1088/0022-3727/9/10/018.
[24] M. Gagné, D. Therriault, Lightning strike protection of composites, Prog. Aerosp. Sci. 64 (2014) 1–16. doi:10.1016/j.paerosci.2013.07.002.
[25] F. A. Fisher, J. A. Plumer, R. A. Perala, Aircraft lightning protection handbook: Dot/faa/ct-89/22 (1989).
[26] A. Brooks, M. Cassissa, S. Halls, Gkn technology: Leading the way toward more efficient aircraft, Presented at Farnborough International Airshow 2014, Farnborough, UK (17 July 2014).
[27] D. Düring, L. Weiß, D. Stefaniak, N. Jordan, C. Hühne, Low-velocity impact response of composite laminates with steel and elastomer protective layer, Compos. Struct. 134 (2015) 18–26. doi:10.1016/j.compstruct.2015.08.001.
[28] C. Hühne, R. Ewert, L. Heinrich, S.-M. Pott-Pollenske, N. Reiche, O. Steffen, Move.on: Multi-optimierung und verifizierung von entwürfen durch performance tests und simulationen : Movable design, optimisation and airframe noise reduction : Abschlussbericht zum teilprojekt des dlr im verbund move.on : Berichtszeitraum: 01.01.2012 bis 30.09.2015 (2016). doi:10.2314/GBV:869875329.
[29] A. Pototzky, Graphenunterstützte konstruktionsmethode zur funktionsintegration in leichtbaustrukturen, Dissertation, Technische Universität Braunschweig, Braunschweig, Germany (2020).
[30] E. Kappel, Process distortions in composite manufacturing: From an experimental characterization to a prediction approach for the global scale, Dissertation, Otto-von-Guericke-Universität Magdeburg, Magdeburg, Germany (2013).
[31] H. Huth, Zum einfluß der nietnachgiebigkeit mehrreihiger nietverbindungen auf die lastübertragungs- und lebensdauervorhersage, Dissertation (1984).
[32] F. Hürlimann, R. Kelm, M. Dugas, G. Kress, Investigation of local load introduction methods in aircraft pre-design, Aerosp. Sci. Technol. 21 (1) (2012) 31–40. doi:10.1016/j.ast.2011.04.008.
[33] M. C.-Y. Niu, Composite airframe structures: Practical design information and data, second edition, fifth published. Edition, Conmilit Press LTD, Hong Kong, 1992.
[34] C. Kassapoglou, Design and analysis of composite structures: With applications to aerospace structures, John Wiley, Chichester, 2010.
[35] O. Steffen, M. Buggisch, J. Kosmann, E. Kappel, H. Köke, C. Hühne, On-ground testing of a laminar flow wing leading edge (2021). doi:10.25967/550045.
[36] C. Uckert, T. Bach, E. Kappel, L. Heinrich, O. Steffen, Cfrp upper wing cover for natural laminar flow, Presented at 27th SICOMP Conference on Manufacturing & Design of Composites, Linköping, Sweden (30-31 May 2016).
URL https://elib.dlr.de/105741/
[37] [link].
URL http://www.midaco-solver.com/
[38] M. Bock, M. Kleineberg, Assembly 4.0 - flexibly picked up, precisely mounted, SAE Int. J. Adv. & Curr. Prac. in Mobility 1 (2) (2019) 352–356. doi:10.4271/2019-01-1355.
[39] O. Steffen, Influence of design and production parameters on the geometrical quality of an aircraft leading edge for natural laminar flow, Presented at 6th Aircraft Structural Design Conference, Bristol, UK (09-11 October 2018).
[40] D. Stefaniak, Improving residual strength of unidirectionally reinforced plastic laminates by metal layering, Dissertation, Technische Universität Braunschweig, Braunschweig, Germany (2017).
[41] M. Buggisch, Entwicklung eines fertigungsprozesses für eine laminare

flügelvorderkante, Presented at Deutscher Luft- und Raumfahrtkongress 2021, Bremen, Germany and Online (31 August - 2 September 2021).
[42] S. Dähne, O. Steffen, J. Kosmann, C. Hühne, An automated assessement tool of nlf criteria for airframe joints (2022). doi:10.25967/570041.
[43] L. Heinrich, M. Kruse, Laminar composite wing surface waviness - two counteracting effects and a combined assessment by two methods (2016). URL https://www.dglr.de/publikationen/2016/420148